

# Critical Temperature and Thermodynamics of Attractive Fermions at Unitarity

Evgeni Burovski,<sup>1</sup> Nikolay Prokof'ev,<sup>1,2,3</sup> Boris Svistunov,<sup>1,2</sup> and Matthias Troyer<sup>4</sup>

<sup>1</sup>*Department of Physics, University of Massachusetts, Amherst, MA 01003*

<sup>2</sup>*Russian Research Center "Kurchatov Institute", 123182 Moscow, Russia*

<sup>3</sup>*Dipartimento di Fisica, Università di Trento and BEC-INFM, I-38050 Povo, Italy*

<sup>4</sup>*Institut für theoretische Physik, ETH Zürich, CH-8093 Zürich, Switzerland*

The unitarity regime of the BCS-BEC crossover can be realized by diluting a system of two-component lattice fermions with an on-site attractive interaction. We perform a systematic-error-free finite-temperature simulations of this system by diagrammatic determinant Monte Carlo. The critical temperature in units of Fermi energy is found to be  $T_c/\varepsilon_F = 0.152(7)$ . We also report the behavior of the thermodynamic functions, and discuss the issues of thermometry of ultracold Fermi gases.

PACS numbers: 03.75.Ss, 05.10.Ln, 71.10.Fd

The unitarity limit is commonly referred to as the limit of a diverging scattering length  $a \rightarrow \infty$ , and an effective range of the interaction  $r_e \rightarrow 0$ . A Fermi gas in this limit attains universality: at low enough temperature the only relevant length scale is given by the density,  $n$ , since the divergent scattering length drops out completely and the system's properties are independent of the interaction details. The unitarity limit is approximately realized in the inner crust of the neutron stars, where the neutron-neutron scattering length is nearly an order of magnitude larger than the mean interparticle separation [1]. Unitarity conditions can also be achieved with cold trapped atom gases using the Feshbach resonance technique, *i.e.* tuning the scattering length to infinity using the magnetic field. In recent years these systems have been extensively studied experimentally [2, 3].

In the limit of  $\xi = 1/na^3 \rightarrow +\infty$  the fermions pair into bosonic molecules and form a Bose-Einstein condensate (BEC). In the opposite limit  $\xi \rightarrow -\infty$  one recovers the Bardeen-Cooper-Schrieffer (BCS) limit. The unitarity limit  $\xi \rightarrow 0$  separates these two extremes. In all these cases, a gas undergoes a superfluid (SF) phase transition at some temperature, which depends on  $\xi$ .

The early analytical treatments of the unitary Fermi gas have been based on the extension of the BCS-type many-body wave function [4]. Most of the subsequent elaborations are also of mean-field type (with or without fluctuations) [5, 6, 7, 8, 9, 10]. The accuracy and reliability of such approximations is nevertheless questionable given the strongly interacting nature of the unitarity regime, and the results differ by nearly an order of magnitude.

Monte Carlo (MC) simulations of Fermi systems are, in general, severely hindered by a sign problem [11]. Fortunately for fermions with attractive contact interaction the sign problem can be avoided [12, 13, 14]. The ground state of a unitary Fermi gas has been studied within a fixed-node MC framework [15], the systematic errors of which depend on the quality of a guess of the nodal structure of a many-body fermion configuration. Despite a

number of calculations at finite temperatures [16, 17, 18], a reliable estimate of the critical temperature is lacking. The purpose of this Letter is to provide accurate results for the critical temperature and thermodynamic functions of a three-dimensional (3D) unitary Fermi gas using a novel determinant diagrammatic MC method free of systematic errors.

Consider an attractive Hubbard model (AHM) defined by the Hamiltonian  $H = H_0 + H_1$ , with

$$H_0 = \sum_{\mathbf{k}\sigma} (\epsilon_{\mathbf{k}} - \mu) c_{\mathbf{k}\sigma}^\dagger c_{\mathbf{k}\sigma}, \quad H_1 = -U \sum_{\mathbf{x}} n_{\mathbf{x}\uparrow} n_{\mathbf{x}\downarrow}, \quad (1)$$

where  $c_{\mathbf{k}\sigma}^\dagger$  is a fermion creation operator,  $n_{\mathbf{x}\sigma} = c_{\mathbf{x}\sigma}^\dagger c_{\mathbf{x}\sigma}$ ,  $\sigma = \uparrow, \downarrow$  is the spin index,  $\mathbf{x}$  enumerates sites of a 3D simple cubic lattice with periodic boundary conditions, the quasimomentum  $\mathbf{k}$  spans the corresponding Brillouin zone,  $\epsilon_{\mathbf{k}} = -2t \sum_{\alpha=1}^3 \cos k_\alpha$  is the tight-binding spectrum,  $t = 1$  is the hopping amplitude,  $\mu$  stands for the chemical potential,  $U > 0$  is the on-site attraction, and we have set the lattice spacing to unity.

By solving the two-body problem of the model (1) one finds that the scattering length diverges at  $U_c = (L^{-3} \sum_{\mathbf{k} \in \text{BZ}} 1/2\epsilon_k)^{-1} \approx 7.915t$ . We use this value of  $U$  throughout. Since we are ultimately interested in the continuum rather than lattice results, we study the low density limit  $\nu \rightarrow 0$ , where  $0 \leq \nu \leq 2$  is the filling fraction. We define Fermi momentum as  $k_F = (3\pi^2\nu)^{1/3}$  and Fermi energy  $\varepsilon_F = k_F^2$ , as those of a continuum gas with the same effective mass and number density  $n = \nu$ .

We simulate the model (1) by diagrammatic determinant MC, discussed in detail in Refs. [13, 19]. One starts by expanding  $\exp(-\beta H)$  in the interaction representation in powers of  $H_1$ . The resulting Feynmann diagrams consist of four-point vertices representing the Hubbard interaction, connected by free single-particle propagators. The sum over all possible ways of connecting vertices with propagators, in the  $n$ -th order diagram is represented by a vertex configuration  $\mathcal{S}_n = \{(\mathbf{x}_j, \tau_j), j = 1, \dots, n\}$ , where  $\tau$  is the imaginary time, see Fig. 1 .

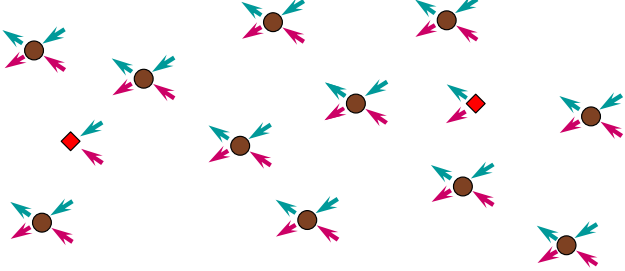


FIG. 1: A sketch of a vertex configuration for the correlation function. Brown dots are the four-point vertices, with the incoming and outgoing lines shown. Red diamonds represent the two-point vertices corresponding to  $P(\mathbf{x}, \tau)$  and  $P^\dagger(\mathbf{x}', \tau')$ . See the text for discussion.

In case of equal number of spin-up and spin-down particles, the differential weight of a configuration is positive definite:

$$d\mathcal{P}(\mathcal{S}_n) = U^n |\det \mathbf{A}(\mathcal{S}_n)|^2 \prod_{j=1}^n d\tau_j, \quad (2)$$

where  $\mathbf{A}(\mathcal{S}_n)$  is an  $n \times n$  matrix built on single-particle propagators:  $A_{ij} = G^{(0)}(\mathbf{x}_i - \mathbf{x}_j, \tau_i - \tau_j)$ .

The configuration space is sampled with worm-type [20] updating scheme [21], based on the two-particle correlation function

$$G_2(\mathbf{x}, \tau; \mathbf{x}', \tau') = \langle \mathcal{T}_\tau P(\mathbf{x}, \tau) P^\dagger(\mathbf{x}', \tau') \rangle \mathcal{N}^{-2}, \quad (3)$$

where  $\mathcal{T}_\tau$  is the  $\tau$ -ordering,  $P(\mathbf{x}, \tau) = c_{\mathbf{x}\uparrow}(\tau) c_{\mathbf{x}\downarrow}(\tau)$  is the pair annihilation operator, a normalization factor  $\mathcal{N} = \beta L^3$  is introduced for future convenience ( $\beta$  is an inverse temperature), and  $\langle \dots \rangle$  is the thermal average. The non-zero asymptotic value of  $\iint d\tau d\tau' G_2(\mathbf{x}, \tau; \mathbf{x}', \tau')$  as  $|\mathbf{x} - \mathbf{x}'| \rightarrow \infty$  is proportional to the condensate density.

Fig. 1 shows a sketch of a vertex configuration, which features a pair of two-point vertices associated with  $P(\mathbf{x}, \tau)$  and  $P(\mathbf{x}', \tau')$ .

The typical number of vertices in a configuration scales with the system volume as  $M \propto \beta U L^3$ . Thus the Metropolis acceptance ratios for the updates involve the ratio of *macroscopically large* determinants  $\det \mathbf{A}(\mathcal{S}_{n'}) / \det \mathbf{A}(\mathcal{S}_n)$  with  $n' = n$  or  $n \pm 1$ . Since we only need ratios of determinants, fast-update formulas [13] can be used to reduce the computational complexity of an update from  $M^3$  down to  $M^2$ .

We validate our method by comparing results against the exact diagonalization data for a  $4 \times 4$  cluster [22], and simulations of a critical temperature at quarter filling [23, 24]. In both cases we find agreement within a few percent accuracy.

We work in the grand canonical ensemble at fixed  $(L, T, \mu)$ . Extracting the unitarity limit critical temperature,  $T_c$ , for the continuum gas from the lattice sim-

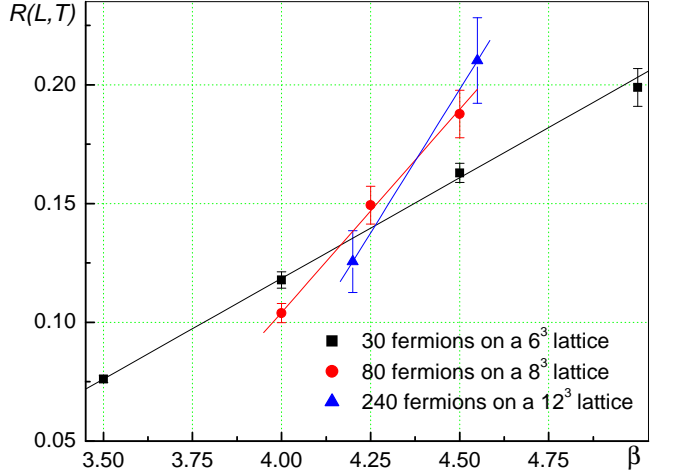


FIG. 2: A typical crossing of the  $R(L, T)$  curves. The errorbars are  $2\sigma$ , and solid lines are the linear fits to the MC points. The data are for the  $\mu = -5.2t$ , thus  $\nu(T = T_c, L \rightarrow \infty) = 0.148(1)$ .

ulation is a two-stage process: first, we study the thermodynamic limit  $L \rightarrow \infty$  to obtain  $T_c(\nu)$  at a given  $\nu$ , and then extrapolate to the continuum limit  $\nu \rightarrow 0$ .

The first task is performed as follows: we simulate a series of system sizes  $L_1 > L_2 > \dots$  at various temperatures. At the critical point the correlation function (3) decays as a power-law at large distances:  $G_2(\mathbf{x}, \tau; \mathbf{x}', \tau') \propto 1/|\mathbf{x} - \mathbf{x}'|^{1+\eta}$ , where  $\eta$  is an anomalous dimension. Since the transition is expected to belong to the  $U(1)$  universality class, we use  $\eta = 0.038$  [25]. Hence, if one sums and rescales the correlation function (3) according to

$$R(L, T) = L^{1+\eta} \sum_{\mathbf{xx}'} \int_0^\beta d\tau \int_0^\beta d\tau' G_2(\mathbf{x}, \tau; \mathbf{x}', \tau'), \quad (4)$$

the intersection of the curves  $R(L_i, T)$  and  $R(L_j, T)$ , shown in Fig. 2, gives a size-dependent estimate  $T_{L_i, L_j}(\mu)$  for the critical temperature  $T_c(\mu)$  [26]. As  $L \rightarrow \infty$ , the series of  $T_{L_i, L_j}(\mu)$  converges to  $T_c(\mu)$  and one can analyze it using corrections to scaling, to extract its limiting value [11]. Likewise, a linear fit of a size-dependent estimate for the filling factor  $\nu(L; \mu)$  versus  $1/L$  yields the thermodynamic limit filling factor  $\nu(\mu)$ .

The next step is to repeat the procedure for a sequence of  $\mu$  values and extrapolate the resultant series of  $T_c(\nu)$  towards  $\nu \rightarrow 0$  using the leading order form  $T_c(\nu)/\varepsilon_F(\nu) = T_c/\varepsilon_F - \text{const} \cdot \nu^{1/3}$ . This functional form is expected from the analysis of the difference between the scattering  $T$ -matrices on the lattice and in the continuum [21].

Shown in Fig. 3 are the simulation results for the critical temperature at filling factors ranging from 0.95 down to 0.06. We use system sizes up to  $16^3$  sites with up to 300

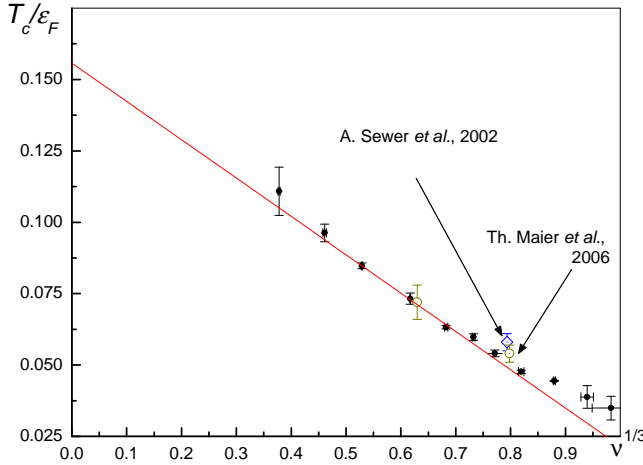


FIG. 3: The scaling of the lattice critical temperature with filling factor (circles). The errorbars are one standard deviation. The results of Ref. [23, 24] at quarter filling are also shown for a comparison. See the text for discussion.

fermions. It is clearly seen that starting from  $\nu \approx 0.5$  the expected  $\nu^{1/3}$  scaling holds very well and the subleading corrections are negligible. On the other hand, close to half-filling,  $T_c(\nu)$  is essentially constant, (see, *e.g.* [27]).

Figure 3 shows a strong dependence of  $T_c(\nu)$  on  $\nu$ . This is in apparent contradiction with Ref. [16] which assumes no such dependence. This might be due to different single-particle spectra  $\epsilon_k$ : Ref. [16] employs a parabolic spectrum with a spherically symmetric cutoff, while we use a tight-binding spectrum over all of the Brillouin zone. Our preliminary tests show that  $\sim \nu^{1/3}$  corrections do depend on the specific choice of single-particle spectrum, and may even have different signs for different  $\epsilon_k$ .

The critical temperature we derive from Fig. 3 is  $T_c = 0.152(7)\varepsilon_F$ . Various approximate schemes have in the past yielded  $T_c$  to be either above [5, 6, 8] or below [7, 9, 10] the BEC limit  $T_{\text{BEC}} = 0.218\varepsilon_F$ . Our results clearly show that it is below.

Previous numerical results were also in disagreement on whether  $T_c$  is higher or lower than  $T_{\text{BEC}}$ : Ref. [17] quotes  $T_c/\varepsilon_F = 0.05$ , but the scattering length has not been determined precisely. Most probably, this result corresponds to a deep BCS regime, where the critical temperature is exponentially suppressed. Lee and Schäfer [18] claim an upper limit  $T_c < 0.14\varepsilon_F$ . This result is based on a study of the caloric curve of a unitary Fermi gas down to  $T/\varepsilon_F = 0.14$  for filling factors down to  $\nu = 0.5$ . The caloric curve of Ref. [18] shows no signs of divergent heat capacity which would signal the phase transition. We find it not surprising since at quarter filling  $T_c(\nu = 0.5)/\varepsilon_F \approx 0.05$ , see Fig. 3. The simulations of Ref. [16], which are also based on a caloric curve study, yield  $T_c = 0.23(2)\varepsilon_F$ . What this otherwise

excellent treatment lacks is an accurate finite-size and finite-density analysis of the MC data.

The value of  $T_c$  determined in this work cannot be directly compared to the experimental result  $T_c = 0.27(2)\varepsilon_F$  [3] for a number of reasons. First, there are strong indications that a presence of a trap significantly enhances the transition temperature, see *e.g.* Ref. [8]. Second, the data analysis of Ref. [3] relies on a mean-field approximate theory for relating the empirical and actual temperature scales. In this regard, it would be extremely interesting to see to what extent the results of Ref. [3] would be affected if a different theoretical scheme is employed for thermometry.

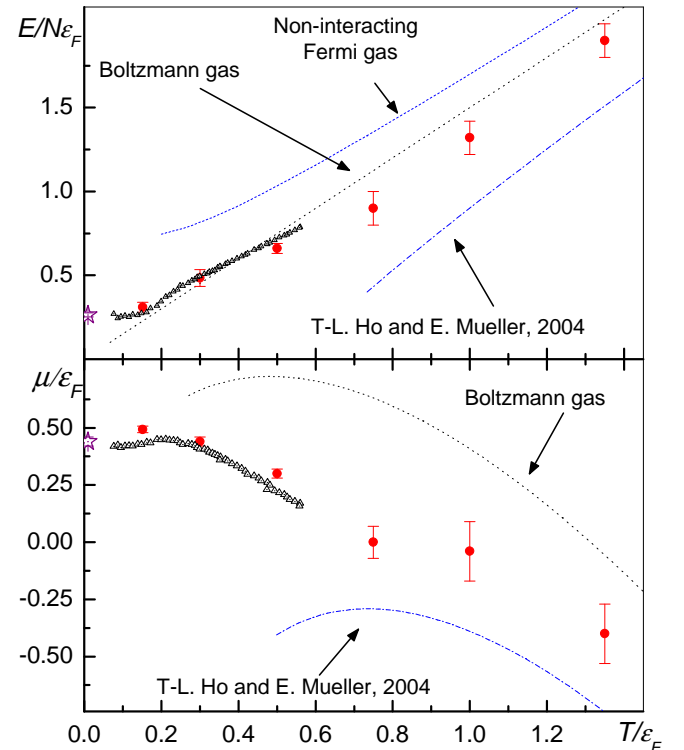


FIG. 4: The temperature dependence of the energy per particle (upper panel) and chemical potential (lower panel) of the unitary Fermi gas. Red circles are the MC results, black dotted lines and blue dashed lines correspond to the Boltzmann and non-interacting Fermi gases, respectively, the dot-dashed lines are the asymptotic prediction of Ref. [29] (plus the first virial Fermi correction), black triangles are the path integral MC results of Ref. [16], and the purple stars denote the ground-state fixed-node MC results [15].

At unitarity, the thermodynamic functions acquire a self-similar form [28]. For example, for the free energy one has:

$$F(T, V, N) = f^{(F)}(T/\varepsilon_F)N\varepsilon_F, \quad (5)$$

where  $N$  is the number of particles,  $V$  is the volume, and  $f^{(F)}(x)$  is a dimensionless function. Eq. (5) allows one to express all thermodynamic potentials in terms of

energy per particle  $f^{(E)} = E/N\varepsilon_F$  and rescaled chemical potential  $f^{(\mu)} = \mu/\varepsilon_F$ . The latter quantities are directly measurable numerically.

An analysis similar to the calculation of  $T_c$  yields

$$E/(N\varepsilon_F) = 0.31(1), \quad (6)$$

$$\mu/\varepsilon_F = 0.493(14). \quad (7)$$

For the pressure  $P$  and entropy  $S$ , one than has

$$P/(n\varepsilon_F) = 0.207(7), \quad (8)$$

$$S/N = 0.16(2), \quad (9)$$

which follows from (7) and exact relations  $PV = (2/3)E$  and  $S = (5E/3 - \mu N)/NT$ . Eqs. (7)-(9) are for  $T = T_c$ .

Shown in Fig. 4 are our results for the dependence of the energy per particle and chemical potential on temperature. In the high-temperature simulations we use system sizes of up to  $32^3$  sites with up to 80 fermions.

As can be seen in Fig. 4, our results for both energy and chemical potential approach values close to the fixed-node MC values [15] as  $T \rightarrow 0$ . For  $T/\varepsilon_F \leq 0.5$  our results are not far from the curve of Ref. [16]. As  $T/\varepsilon_F \rightarrow \infty$ , both energy and chemical potential approach the virial expansion [29] at high temperatures.

In conclusion, we have performed a determinant diagrammatic MC simulations of a unitary Fermi gas by means of diluting the attractive Hubbard model. In order to extract the continuum gas behaviour we carefully treat both finite-size and lattice corrections. We have determined the critical temperature  $T_c/\varepsilon_F = 0.152(7)$ , the values of the thermodynamic functions at criticality, and the overall shape of the thermodynamic potentials from zero- to high-temperature regimes.

We thank A. Bulgac, P. Magierski and J. Drut for providing us with their data. This research was enabled by computational resources of the Center for Computational Sciences and in part supported by the Laboratory Research and Development program at Oak Ridge National Laboratory. Part of the simulations were performed on the “Hreidar” cluster of ETH Zürich. We also acknowledge partial support by NSF grants Nos. PHY-0426881 and PHY-0456261 and by the Swiss National Science Foundation.

*et al.*, Phys. Rev. Lett. **91**, 240402 (2003); M.W. Zwierlein *et al.*, Phys. Rev. Lett. **91**, 250401 (2003); M. Greiner *et al.*, Nature **426**, 537 (2003); S. Jochim *et al.*, Science **302**, 2101 (2003); C.A. Regal *et al.*, Phys. Rev. Lett. **92**, 083201 (2004); M. Bartenstein *et al.*, Phys. Rev. Lett. **92**, 120401 (2004); C.A. Regal *et al.*, Phys. Rev. Lett. **92**, 040403 (2004); M.W. Zwierlein *et al.*, Phys. Rev. Lett. **92**, 120403 (2004); J. Kinast *et al.*, Phys. Rev. Lett. **92**, 150402 (2004); M. Bartenstein *et al.*, Phys. Rev. Lett. **92**, 203201 (2004); C. Chin *et al.*, Science **305**, 1128 (2004); M.W. Zwierlein *et al.*, Nature, **435**, 1047 (2005); G. B. Partridge *et al.*, Science **311**, 503 (2006).

- [3] J. Kinast *et al.* Science **307**, 1296 (2005).
- [4] D.R. Eagles, Phys. Rev **186**, 456 (1969); A.J. Legett, in *Modern Trends in the Theory of Condensed Matter*, eds. A. Pekalski and R. Przystawa (Springer-Verlag, Berlin, 1980).
- [5] P. Nozières and S. Schmitt-Rink, J. Low Temp. Phys. **59**, 195 (1985); M. Randeria, in *Bose-Einstein Condensation*, eds. A. Griffin *et al.* (Cambridge University Press, Cambridge, 1995).
- [6] M. Holland *et al.*, Phys. Rev. Lett. **87**, 120406 (2001); E. Timmermans *et al.*, Phys. Lett. A **285**, 228 (2001).
- [7] Y. Ohashi and A. Griffin, Phys. Rev. Lett. **89**, 103402 (2002).
- [8] A. Perali *et al.*, Phys. Rev. Lett. **92**, 220404 (2004).
- [9] X.-J. Liu and H. Hu, Phys. Rev. A **72**, 063613 (2005).
- [10] R. Haussmann, Phys. Rev. B **49**, 12975 (1994).
- [11] See e.g., K. Binder, D.P. Landau, *A Guide to Monte Carlo Simulations in Statistical Physics* (Cambridge University Press, Cambridge, 2000).
- [12] D.J. Scalapino and R.L. Sugar, Phys. Rev. Lett. **46**, 519 (1981); R. Blankenbecler, D.J. Scalapino, and R.L. Sugar, Phys. Rev. D **24**, 2278 (1981).
- [13] A.N. Rubtsov, cond-mat/0302228; A.N. Rubtsov and A.I. Lichtenstein, Pis'ma v JETP **80**, 67 (2004); A.N. Rubtsov *et al.*, cond-mat/0411344.
- [14] J.-W. Chen and D.B. Kaplan, Phys. Rev. Lett. **92**, 257002 (2004).
- [15] J. Carlson *et al.*, Phys. Rev. Lett. **91**, 050401 (2003); S.-Y. Chang *et al.*, Phys. Rev. A **70**, 043602 (2004); G.E. Astrakharchik *et al.*, Phys. Rev. Lett. **93**, 200404 (2004); Phys. Rev. Lett. **95**, 230405 (2005).
- [16] A. Bulgac *et al.*, Phys. Rev. Lett. **96**, 090404 (2006).
- [17] M. Wingate, cond-mat/050372.
- [18] D.T. Lee and T. Schäfer, nucl-th/0509018.
- [19] E. Burovski, N. Prokof'ev, and B. Svistunov, Phys. Rev. B **70**, 193101 (2004); note that in the present work we do not use the ‘truncation’ idea put forward in this paper.
- [20] N.V. Prokof'ev, B.V. Svistunov, and I.S. Tupitsyn, Phys. Lett. A **238**, 253 (1998).
- [21] E. Burovski, N. Prokof'ev, B. Svistunov, and M. Troyer, in preparation.
- [22] T. Husslein, W. Fettes, and I. Morgenstern, Int. J. Mod. Phys. **C8**, 397 (1997).
- [23] A. Sewer, H. Beck, and X. Zotos, Phys. Rev. B **66**, 140504 (2002).
- [24] T.A. Maier *et al.*, DCA/QMC ,unpublished
- [25] M.E. Fisher, in *Lecture Notes in Physics 186*, Springer-Verlag, 1983.
- [26] K. Binder, Phys. Rev. Lett. **47**, 693 (1981).
- [27] R. Micnas, J. Ranninger, and S. Robaszkiewicz, Rev. Mod. Phys. **62**, 113 (1990).

- [28] T.-L. Ho, Phys. Rev. Lett. **92**, 090402 (2004). (2004).
- [29] T.-L. Ho and E.J. Mueller, Phys. Rev. Lett. **92**, 160404

**Erratum: Critical Temperature and Thermodynamics of Attractive Fermions at Unitarity [Phys. Rev. Lett. 96, 160402 (2006)]**

Evgeni Burovski, Nikolay Prokof'ev, Boris Svistunov, and Matthias Troyer

The value of entropy given in Eq. (9) of Ref. [1] has an incorrect error bar. The correct value is directly related to error bars for energy and chemical potential mentioned in Eqs. (6) and (7) using exact relation  $S/N = (5E/3N - \mu)/T$ . Equation (9) should read:  $S/N = 0.2 \pm 0.2$ , *i.e.* we can not predict the correct value of entropy at the critical point. The loss of precision in the entropy estimate does not affect other results in [1]. However, it precludes quantitative discussion of adiabatic ramp experiments presented in Ref. [2] based on matching entropies of the non-interacting and unitary gases. In particular, the numerical value of  $(T/T_F)^0$  given in Ref. [2] is meaningless.

We thank W. Zwerger for pointing out the issue with the entropy calculation.

---

[1] E. Burovski, N. Prokof'ev, B. Svistunov, and M. Troyer, Phys. Rev. Lett. **96**, 160402 (2006).  
 [2] E. Burovski, N. Prokof'ev, B. Svistunov, and M. Troyer, New J. Phys. **8**, 153 (2006).